

# Massless fermions in multilayer graphitic systems with misoriented layers: *Ab initio* calculations and experimental fingerprints

Sylvain Latil,<sup>1</sup> Vincent Meunier,<sup>2</sup> and Luc Henrard<sup>1</sup>

<sup>1</sup>Laboratoire de Physique du Solide, Facultés Universitaires Notre-Dame de la Paix, rue de Bruxelles 61, 5000 Namur, Belgium

<sup>2</sup>Oak Ridge National Laboratory, Bethel Valley Road, Oak Ridge, Tennessee 37831-6367, USA

(Received 11 September 2007; published 7 November 2007)

We examine how the misorientation of a few stacked graphene layers affects the electronic structure of carbon nanosystems. We present *ab initio* calculations on bilayer and trilayer systems to demonstrate that the massless fermion behavior typical of single-layered graphene is also found in incommensurate multilayered graphitic systems. We also investigate the consequences of this property on experimental fingerprints, such as Raman spectroscopy and scanning tunneling microscopy (STM). Our simulations reveal that STM images of turbostratic few-layer graphite are sensitive to the layer arrangement. We also predict that the resonant Raman signals of graphitic samples are more sensitive to the orientation of the layers than to their number.

DOI: 10.1103/PhysRevB.76.201402

PACS number(s): 81.05.Uw, 71.15.Mb, 73.90.+f

The electronic properties of two-dimensional (2D) graphene and three-dimensional (3D) graphite have been extensively studied for more than 50 years.<sup>1</sup> It is fascinating that the extraordinary properties of carbon nanotubes<sup>2</sup> have been deduced from those of 2D graphene many years before macroscopic samples of very thin few-layer graphite (FLG) could be obtained in the laboratory.<sup>3</sup> A particular interest has been recently given to single layer graphene (SLG) because of its massless fermion behavior, the  $\sqrt{B}$  dependence of the Landau levels,<sup>4,5</sup> and the observation of an abnormal quantum hall effect (QHE), even at room temperature.<sup>6</sup>

In that context, a precise investigation of the layer-to-layer interaction on the existence of massless fermion carriers is of paramount importance. For 3D graphite, the most stable Bernal phase (*AB* stacking) as well as the rhombohedral (*ABC* stacking) shows complex electron and hole bands near the Fermi level rather than linear, massless fermion ones, due to the interlayer interaction.<sup>7</sup> We have recently shown that regular (*AB* or *ABC*) stackings also break the linear character of the dispersion of electronic bands for FLG with two to four layers and that ambipolar electronic conduction could be related to *AB*-stacked FLG.<sup>8</sup>

In this paper, we present an electronic structure analysis of misoriented (turbostratic) two- and three-layer FLG. A recent surface x-ray analysis of multilayer graphene grown on SiC shows that misorientation is plausible.<sup>9</sup> We show here that the linear dispersion of SLG is preserved in turbostratic multilayer systems despite the presence of adjacent layers. It follows that massless fermion carriers are predicted for disoriented multilayer systems. These findings raise the question of the interpretation of the experimental observations performed on FLG samples and challenge the direct relation between SLGs and Dirac massless fermions. More generally, the electronic properties (and consequently the optical, vibrational, and transport properties) of a given FLG film are found to be controlled mainly by the (mis)orientation of the successive layers rather than their number. In the present work, we discuss also the implications of this possible misorientation on experimental signatures, in particular on scanning tunneling microscopy (STM) and Raman fingerprints.

The main technical difficulty when modeling turbostratic

structures is to combine their incommensurate character and the necessary finiteness of the supercell in solid-state calculations. An elegant solution, proposed by Kolmogorov and Crespi,<sup>10</sup> consists in the definition of a graphene hexagonal supercell without mirror symmetry (except the basal plane). The smallest supercell of this type contains 14 atoms and is defined with its basis vectors  $\mathbf{A}_1=2\mathbf{a}_1+\mathbf{a}_2$  [denoted as (2, 1) supercell hereafter] and  $\mathbf{A}_2=-\mathbf{a}_1+3\mathbf{a}_2$ , as shown in Fig. 1. The supercell (3,  $\bar{1}$ ) possesses exactly the same basis vectors, but is rotated by the angle  $\cos^{-1}(11/14) \approx 38.21^\circ$ . When stacking these two supercells, we obtain a bilayer structure with short-range incommensurability (Fig. 1). The (7, 0) and (5, 3) supercells have also the same size but a larger number of atoms (98 C atoms per layer) and can be assembled onto bilayer or trilayer compounds fulfilling the translational symmetry requirements.<sup>11</sup>

Here, we focus our attention on bilayer and trilayer FLG structures based on the (2, 1) and (7, 0)/(5, 3) supercells. Our aim is to highlight significant differences in the band structures of commensurate and incommensurate graphitic systems. All the calculations were performed with density functional theory (DFT), within the local density approximation (LDA) scheme, and using norm-conserving pseudopotentials.<sup>12</sup> Depending on the number of atoms involved in the supercell, the eigenproblem was expanded on plane waves (PWs, using the code ABINIT<sup>13</sup>) or localized pseudoatomic orbitals (PAOs, using the code SIESTA<sup>14</sup>). In

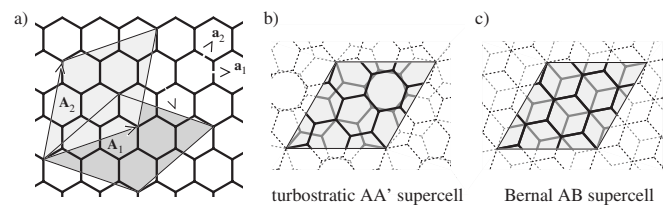


FIG. 1. (a) The nonsymmetric supercell (2, 1) (light gray), and its two primitive vectors  $\mathbf{A}_1$  and  $\mathbf{A}_2$ . The (3,  $\bar{1}$ ) cell is drawn in dark gray. (b) A quasi-incommensurate bilayer AA' structure, made by stacking the (2, 1) on the (3,  $\bar{1}$ ) supercell. (c) An AB bilayer structure supercell.

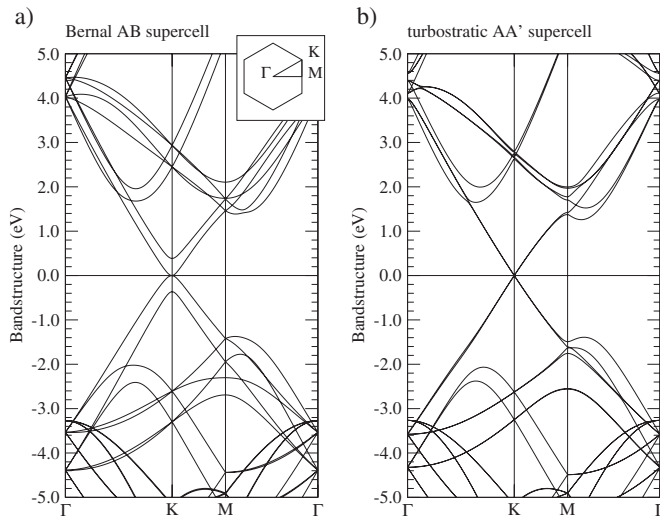


FIG. 2. The 2D electronic band structures of Bernal  $AB$  (a) and turbostratic  $AA'$  (b) bilayer graphene. Both are based on the supercell represented in Fig. 1. The hexagonal Brillouin zone of the system is shown in the inset.

the first case, the plane-wave cutoff energy was set to 35 hartrees. In the second case, the basis was composed of atom-centered double- $\zeta$  functions. Even though the long-range van der Waals coupling is missing in DFT calculations, it has been shown that the LDA yields accurate interlayer equilibrium distances in graphitic systems<sup>10</sup> and describes correctly the electronic structure near  $E_F$  of 3D graphite<sup>7</sup> and FLG.<sup>8,15</sup>

We first carried out a structural optimization of each bilayer (2,1)-based supercell (PW calculations with tolerance for the forces set to  $10^{-6}$  hartree/bohr and a  $12 \times 12 \times 1$  grid sampling of the Brillouin zone). No significant atomic rearrangement is observed within a plane, the only structural reorganization taking place in the average interlayer distance (3.33 Å for the  $AB$  and 3.42 Å for the turbostratic stacked bilayer). The corresponding band structures of the two (2,1)-based bilayers are plotted in Fig. 2. We have carefully verified that PAO basis yields identical results.

Figure 2(a) reproduces the well-known results for an  $AB$  bilayer<sup>8,16</sup> within a supercell  $\sqrt{7} \times \sqrt{7}$  larger than the primitive cell and is displayed for comparison. As in previously published calculations, we notice a  $\sim 0.8$ -eV splitting of the electronic bands, related to the layer-layer interactions in the  $AB$  geometry. The bilayer graphene with a  $38.21^\circ$  misorientation (called  $AA'$  hereafter) presents a totally different signature near the Fermi level [Fig. 2(b)]. Surprisingly, the band structure here is found to be similar to the one of SLG but doubly degenerate. The significance of this result is striking, since a massless fermion character is found for misoriented bilayer systems with a Fermi velocity of  $\sim 9.6 \times 10^6$  m s<sup>-1</sup>, strictly identical to the value deduced for SLG within the same formalism and similar to experimental values.<sup>6,22</sup> We have checked that this unexpected behavior is also found in the turbostratic (5,3)-on-(8, $\bar{3}$ ) bilayer that presents a misorientation angle of  $43.57^\circ$  (Ref. 17). The apparent absence of an interaction between layers at the Fermi level can be related to the loss of short-range correlation between successive layers.

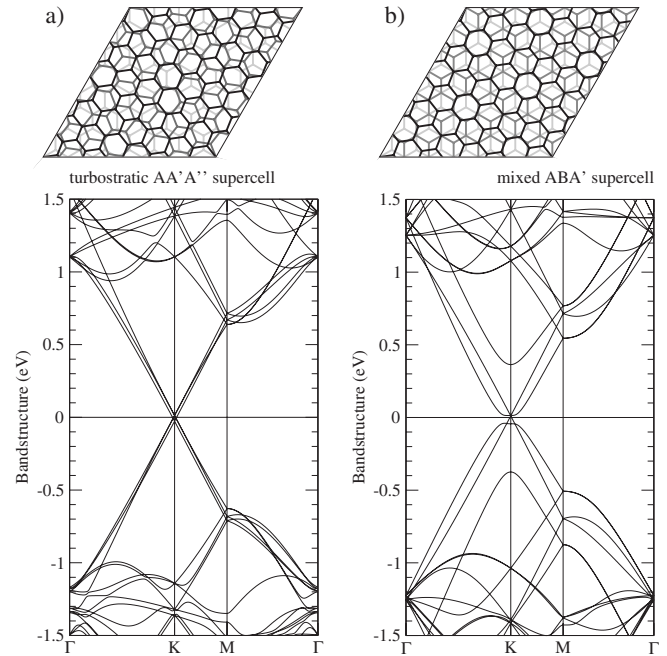


FIG. 3. Representation of the supercells and the corresponding electronic band structure for trilayer graphites. The turbostratic  $AA'A''$  system ( $43.57^\circ$  and  $38.21^\circ$  misorientation angles) is shown in (a), and the mixed  $ABA'$  structure is shown in (b).

Turning to the trilayer FLG system, we use the interlayer distance found for bilayer cases, depending on the stacking geometry ( $AB$  or turbostratic). The PAO electronic calculations shown here have been checked against PW calculations. In Fig. 3, we present the results for a purely  $AA'A''$  turbostratic (5,3)-on-(8, $\bar{3}$ )-on-(7,0) trilayer with two respective misorientations of  $43.57^\circ$  and  $38.21^\circ$  and for a mixed case (5,3)-on-( $\bar{7}$ ,0)-on-(7,0), made from a bilayer with  $AB$  stacking and a third one misoriented ( $38.21^\circ$ ), called  $ABA'$ . The results for the calculation for  $ABA$  or  $ABC$  stacking can be found in Refs. 8 and 18.

The trilayer with a mixed stacking  $ABA'$  displays electronic bands [Fig. 3(b)] similar to a superposition of an  $AB$  bilayer [Fig. 2(a)] and a single-layer graphene (linear dispersion). The band crossing of the graphenelike bands lies 12 meV above the Fermi level, indicating a small charge transfer of  $\sim 10^{11} e$  cm<sup>-2</sup>. The other (quadratic) bands present a gap opening that is consistent with the behavior found for  $AB$  bilayer graphene under an electric field.<sup>18</sup> We have checked that the same systems but with the  $A'$  layer away from its equilibrium position present a vanishing small charge transfer—i.e., a progressive closure of the “gap” of the quadratic bands and a Dirac point of the linear bands moving towards the Fermi level. Interestingly, the turbostratic  $AA'A''$  trilayer follows the trends observed for the bilayer and displays linearly dispersive bands and massless fermion behavior. The (doubly degenerate) bands associated with the external layers are slightly shifted upward ( $\sim 12$  meV) while the bands related to the central layer are slightly shifted downward ( $\sim 25$  meV). This is also the signature of a small electron transfer, from the external layers to

the central one, consistent with the previous  $ABA'$  case. We have also checked that the deviation from the linear dispersion of the  $\pi$  bands for  $|E| > 0.5$  eV is mainly due to the trigonal warping effect of graphene and not to an interlayer effect.

The results presented above demonstrate that turbostratic stacking of graphene sheets leads to a linear dispersion of the electronic levels similar to the behavior of SLG. Furthermore, the mixed stacking case shows a superposition of the two types of carriers—i.e., a massless fermion and a massive, normal electronic behavior. Consequently, direct experimental evidence of Dirac fermion behavior cannot be considered as a discriminating property between single-layer and multilayer systems. In particular, the number of  $\pi$  bands in angle-resolved photoemission spectroscopy (ARPES) measurement<sup>19</sup> is not enough to determine the number of layers.

The absence of a net effect of the interlayer interaction on the electronic dispersion of turbostratic FLG also suggests that the  $\sqrt{B}$  dependence of the Landau levels can also occur for multilayer structures and that the abnormal QHE cannot be excluded. Remarkably, this consequence of our study is supported by recent experimental data. First,  $\sqrt{B}$  Landau-level separation has been observed in three to five graphene layers grown on SiC substrate.<sup>5</sup> Second, Dirac fermion behavior, integer QHE,<sup>20</sup> and infrared probe anomalous magnetotransport have been also reported in a highly ordered pyrolytic graphite (HOPG) bulk 3D sample.<sup>21</sup>

Recently, the observation of a single 2D band ( $\sim 2700$   $\text{cm}^{-1}$ ) in Raman spectroscopy has been proposed as experimental evidence for the determination of the number of layers in FLG samples.<sup>16,23,24</sup> For two-layer (and thicker) films, the interlayer interaction induces a splitting of the electronic bands. This means that in a double-resonance Raman process, the resulting effect is a splitting of this 2D peak.<sup>16,24</sup> Our results show that the effect of the interlayer interaction on the splitting of the electronic bands crucially depends on the relative orientation of the layers and not only on the number of layers. The conclusion of Refs. 16 and 24 remains valid only for  $AB$ -stacked film but cannot be generalized for all FLG systems. For instance, since a turbostratic bilayer possesses degenerate electronic bands near the Fermi level, the 2D mode of this structure gives rise to a single peak that is indistinguishable from the signature of SLG systems. Similarly, a trilayer turbostratic structure will also present a single 2D band. Indeed, as we have discussed above, the splitting of the electronic bands in that case is due to a charge transfer and no evidence of covalent mixing has been found. The 2D peak of the mixed  $ABA'$  trilayer will present three main features. Two of them are associated with the  $AB$ -like bands, the third one with the  $A'$  layer, identical to the SLG case.

Interestingly, the splitting of the 2D band of graphitic materials has been found to be a good criterion of crystallinity perpendicular to the basal planes. For instance, in Ref. 25, the authors have correlated the interlayer distance in bulk graphite with the doubling of the 2D band, finding that for  $d > 0.338$  nm a single 2D band is observed where a double 2D band is observed for  $d < 0.338$  nm. From these findings and the results presented here, we can predict that HOPG

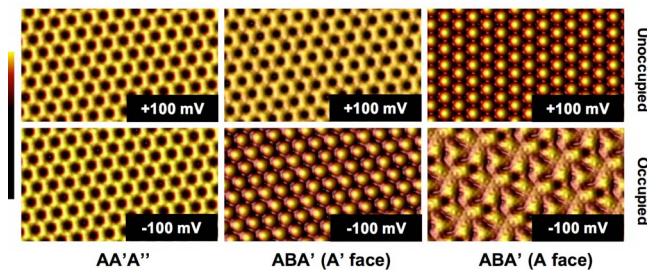


FIG. 4. (Color online) From left to right: constant-current STM image simulation of turbostratic  $AA'A''$  and mixed  $ABA'$  systems. (Un)occupied states are images at (positive) negative tip potential. The color scale spans the corrugation of each system: 1.6 (1.4) Å, 2.3 (2.4) Å, and 1.8 (2.1) Å for each system at positive (negative) bias.

graphite with disorder in the staking (and large  $d$ ) will present a single 2D line whereas Bernal graphite with (partial)  $AB$  order will present a doubling of the 2D line. From this discussion, it is clear that an unequivocal determination of the number of layers is not possible from Raman spectroscopy alone.

We now analyze the STM images of the trilayer systems studied above. Recent experimental data on monolayer and bilayer graphite on SiC substrate show a  $\sqrt{3} \times \sqrt{3}$  modulation of the STM intensity. This effect has been associated with the substrate reconstruction<sup>15,26,27</sup> rather than to the relative arrangement of the graphitic layers. Here, we have computed the STM images of trilayer systems without the substrate in order to discriminate the intrinsic response of FLG from the effect of interaction with the substrate. This approach is made possible by the prerequisite of Tersoff-Hamann theory since the image formation is governed by integration of local density of states and does not require a closed circuit to simulate the current.<sup>28</sup> Here we made use of the BSKAN package implementation of Tersoff-Hamann theory.<sup>29,30</sup> Constant current images for systems represented in Fig. 3 are shown in Fig. 4 for positive and negative tip polarities. For system  $ABA'$  the two external faces are not equivalent and the corresponding images are given for both faces. At low bias (100 mV was used here), the images reflect the property of the states close to the Fermi level. For system  $AA'A''$ , both positive and negative bias images look the same, with all the atoms being imaged, just as in SLG. The situation is quite different for  $ABA'$  systems. The image for occupied states of the  $A'$  face shows bright spots on every other atom, while a complete honeycomb lattice is imaged for unoccupied states. The situation is even more complicated for images computed on the  $A$  face of the  $ABA'$  system. While every other atom is now revealed at tip bias corresponding to unoccupied states, the occupied state image clearly shows a small-scale moiré-like pattern. It is important to note that the images have been simulated for zero-temperature conditions: given the very small energy difference between the states responsible for the images at low bias, the room-temperature image will most probably look like an average of the images reproduced here.

In summary, we found that, as a consequence of the incommensurability of the layers, multilayer graphitic systems possess a massless fermion carriers property. Since that property was up to now considered as a unique signature of single-layer graphene, the present findings challenge the interpretation of the experimental data on FLG and highlight the crucial role of the relative orientation of the graphitic layers, related to the production methods (for example, mis-oriented film signature have been observed only on SiC grown films<sup>31</sup>). Our findings also release the restriction of

using single-layer graphene to build devices based on the on massless fermion feature.

Calculations were performed at the Namur Interuniversity Scientific Computing Facility (I-SCF), a common project between the FRS-FNRS and the University of Namur. S.L. and L.H. acknowledge financial support from the Belgian FRS-FNRS. V.M. acknowledges the Division of Materials Sciences, U.S. Department of Energy, under Contract No. DEAC05-00OR22725 with UT Battelle, LLC at ORNL.

- <sup>1</sup>J. W. McClure, Phys. Rev. **108**, 612 (1957); J. C. Slonczewski and P. R. Weiss, *ibid.* **109**, 272 (1958).
- <sup>2</sup>J.-C. Charlier, X. Blase, and S. Roche, Rev. Mod. Phys. **79**, 677 (2007).
- <sup>3</sup>K. S. Novoselov, A. K. Geim, S. V. Morozov, D. Jiang, Y. Zhang, S. V. Dubonos, I. V. Grigorieva, and A. A. Firsov, Science **306**, 666 (2004); C. Berger, Z. Song, T. Li, X. Li, A. Y. Ogbazghi, R. Feng, Z. Dai, A. N. Marchenkov, E. H. Conrad, P. N. First, and W. de Heer, J. Phys. Chem. B **108**, 19912 (2004).
- <sup>4</sup>V. P. Gusynin and S. G. Sharapov, Phys. Rev. B **73**, 245411 (2006).
- <sup>5</sup>M. L. Sadowski, G. Martinez, M. Potemski, C. Berger, and W. A. de Heer, Phys. Rev. Lett. **97**, 266405 (2006).
- <sup>6</sup>K. S. Novoselov, A. K. Geim, S. V. Morozov, D. Jiang, M. I. Katsnelson, I. V. Grigorieva, S. V. Dubonos, and A. A. Firsov, Nature (London) **438**, 197 (2005); V. P. Gusynin and S. G. Sharapov, Phys. Rev. Lett. **95**, 146801 (2005); Y. Zhang, Y.-W. Tan, H. L. Stormer, and P. Kim, Nature (London) **438**, 201 (2005); K. S. Novoselov, Z. Jiang, Y. Zhang, S. V. Morosov, H. L. Stormer, U. Zeittler, J. C. Maan, G. S. Boebinger, P. Kim, and A. K. Geim, Science **315**, 1379 (2007).
- <sup>7</sup>J.-C. Charlier, X. Gonze, and J.-P. Michenaud, Phys. Rev. B **43**, 4579 (1991); Carbon **92**, 289 (1994).
- <sup>8</sup>S. Latil and L. Henrard, Phys. Rev. Lett. **97**, 036803 (2006).
- <sup>9</sup>J. Hass, R. Feng, J. E. Millan-Otoya, X. Li, M. Sprinkle, P. N. First, W. A. de Heer, E. H. Conrad, and C. Berger, Phys. Rev. B **75**, 214109 (2007).
- <sup>10</sup>A. N. Kolmogorov and V. H. Crespi, Phys. Rev. B **71**, 235415 (2005).
- <sup>11</sup>It is impossible to create a totally misoriented trilayer structure based on the (2,1) supercell, which is still compatible with the translational symmetry requirements.
- <sup>12</sup>N. Troullier and J. L. Martins, Phys. Rev. B **43**, 8861 (1991).
- <sup>13</sup>X. Gonze, J. M. Beuken, R. Caracas, F. Detraux, M. Fuchs, G. M. Rignanese, L. Sindic, M. Verstraete, G. Zerah, F. Jollet, M. Torrent, A. Roy, M. Mikami, P. Ghosez, J. Y. Raty, and D. C. Allan, Comput. Mater. Sci. **25**, 478 (2002).
- <sup>14</sup>J. M. Soler, E. Artacho, J. D. Gale, A. Garcia, J. Junquera, P. Ordejon, and D. Sanchez-Portal, J. Phys.: Condens. Matter **14**, 2745 (2002).
- <sup>15</sup>F. Varchon, R. Feng, J. Hass, X. Li, B. N. Nguyen, C. Naud, P. Mallet, J.-Y. Veuillen, C. Berger, E. H. Conrad, and L. Magaud, Phys. Rev. Lett. **99**, 126805 (2007).
- <sup>16</sup>D. Graf, F. Molitor, K. Ensslin, C. Stampfer, A. Jungen, C. Hierold, and L. Wirtz, Nano Lett. **7**, 238 (2007).
- <sup>17</sup>This result has been confirmed very recently for the (3,1) supercell based bilayers: J. Hass, F. Varchon, J. E. Millan-Otoya, M. Sprinkle, W. A. de Heer, C. Berger, P. N. First, L. Magaud, and E. H. Conrad, e-print arXiv:cond-mat/0706.2134.
- <sup>18</sup>M. Aoki and H. Amawashi, Solid State Commun. **142**, 123 (2007).
- <sup>19</sup>T. Ohta, A. Bostwick, T. Seyller, K. Horn, and E. Rotenberg, Science **313**, 951 (2006); T. Ohta, A. Bostwick, J. L. McChesney, T. Seyller, K. Horn, and E. Rotenberg, Phys. Rev. Lett. **98**, 206802 (2007); A. Bostwick, T. Ohta, T. Seyller, K. Horn, and E. Rotenberg, Nat. Phys. **3**, 36 (2007).
- <sup>20</sup>H. Kempa, P. Esquinazi, and Y. Kopelevich, Solid State Commun. **138**, 118 (2006).
- <sup>21</sup>Z. Q. Li, S.-W. Tsai, W. J. Padilla, S. V. Dordevic, K. S. Burch, Y. J. Wang, and D. N. Basov, Phys. Rev. B **74**, 195404 (2006); G. Li and E. Y. Andrei, Nat. Phys. **3**, 623 (2007).
- <sup>22</sup>I. A. Luk'yanchuk and Y. Kopelevich, Phys. Rev. Lett. **97**, 256801 (2006); S. Y. Zhou, G.-H. Gweon, J. Graf, A. V. Fedorov, C. D. Spataru, R. D. Diehl, Y. Kopelevich, D.-H. Lee, S. G. Louie, and A. Lanzara, Nat. Phys. **2**, 595 (2007).
- <sup>23</sup>A. Gupta, G. Chen, P. Joshi, S. Tadigadapa, and P. C. Eklund, Nano Lett. **6**, 2667 (2006).
- <sup>24</sup>A. C. Ferrari, J. C. Meyer, V. Scardaci, V. Casiraghi, M. Lazzeri, F. Mauri, S. Piscanec, D. Jiang, K. S. Novoselov, S. Roth, and A. K. Geim, Phys. Rev. Lett. **97**, 187401 (2006).
- <sup>25</sup>P. Lespade, A. Marchand, M. Couzi, and F. Cruege, Carbon **22**, 375 (1984).
- <sup>26</sup>G. M. Rutter, J. N. Crain, N. P. Guisinger, T. Li, P. N. First, and J. A. Stroscio, Science **317**, 21 (2007).
- <sup>27</sup>P. Mallet, F. Varchon, C. Naud, L. Magaud, C. Berger, and J. Y. Veuillen, Phys. Rev. B **76**, 041403(R) (2007).
- <sup>28</sup>J. Tersoff and D. R. Hamann, Phys. Rev. B **31**, 805 (1985).
- <sup>29</sup>W. A. Hofer and J. Redinger, Surf. Sci. Rep. **447**, 51 (2000).
- <sup>30</sup>For convenience, the DFT charge density used for STM simulations was obtained using the plane-wave VASP package [G. Kresse and J. Hafner, Phys. Rev. B **47**, 558 (1993); G. Kresse and J. Furthmuller, Comput. Mater. Sci. **6**, 15 (1996); G. Kresse and J. Furthmuller, Phys. Rev. B **54**, 11169 (1996)], which can be readily used for STM simulations. The same parameters for VASP as for ABINIT calculations were used as described in the text, yielding identical results.
- <sup>31</sup>W. A. de Heer, C. Berger, X. Wu, P. N. First, E. H. Conrad, X. Li, T. Li, M. Sprinkle, J. Hass, M. L. Sadowski, M. Potemski, and G. Martinez, Solid State Commun. **143**, 92 (2007).